Materials Science Forum Vols. 798-799 (2014) pp 391-395

doi:10.4028/www.scientific.net/MSF.798-799.391

Preparation of porous zirconia-yttria ceramics by thermal removal of potassium iodide

Sabrina G. M. Carvalho[a], R. Muccillo[b]

Center of Science and Technology of Materials, Energy and Nuclear Research Institute

Travessa R 400, Cidade Universitaria, S. Paulo, SP, Brazil 05508-900

[a]sabrina.carvalho@usp.br, [b]muccillo@usp.br

Keywords: porous ceramics, zirconia-yttria.

Abstract. Zirconia-8 mol% yttria porous solid electrolytes were obtained by mixing with different amounts (0 to 5 wt.%) of KI prior to sintering. Potassium iodide acts as sacrificial pore former, being removed from the ceramic pellet upon sintering at 1400 ^{o}C/2 h. The alkali halide content was evaluated by X-ray fluorescence analysis, the density of the pellets by the Archimedes method, and the pore content by observation in scanning probe (SPM) and scanning electron (SEM) microscopes of polished and etched surfaces. The oxide ion resistivity was determined by impedance spectroscopy analysis in the 5 Hz-13 MHz frequency range from 300 to 500 ^{o}C. Porous specimens with high skeletal density were obtained. The higher is the alkali halide content, the higher is the pore volume and the total electrical resistivity. A correlation is found between the pore content, evaluated by SEM and SPM, and the electrical behavior analysis from the impedance plots of the porous specimens.

Introduction

ZrO_2:8 mol% Y_2O_3 polycrystalline ceramics, having high ionic conductivity above room temperature, are widely used in oxygen sensors and in solid oxide fuel cells as dense electrolytes or part of porous anode. Porous ceramics must have high skeletal density for supporting mechanical strength under operation. The processing of porous ceramics is important to obtain suitable properties like pore density, average pore size, pore distribution and pore connectivity [1]. Sol-gel synthesis, the use of sacrificial organic pore formers which are eliminated upon calcination [2,3], and templates of polymeric foams are the main approaches for obtaining porous ceramics. The evaluation of porosity in ceramics is usually carried out by mercury porosimetry intrusion or by observation od fracture surfaces in optical or electron microscopes. The electrical behavior of porous ceramics differs from that of dense ceramics. Pores may be considered volume defects impeding charge transport, acting as blockers [4-6] to charge carriers. The electric current lines due to the application of an electric field make a detour around the pores, producing a modification in the impedance plots of the solid electrolytes in the low frequency region (intergranular response). In other words, the mean free path of the charge carriers through the ceramic body under an electric field is larger in a porous region than in a dense region. This behavior has already been reported for cracks in zirconia-based solid electrolytes [7] and in porous zirconia-yttria ceramics [8]. The preparation of suitable materials for SOFC devices remains a challenge in Materials Science. The decrease in the operational temperature of SOFCs to 650 ^{o}C will effectively help the commercialization of these devices [9]. The suitable porosity for anodes in SOFCs is approximately 40% [10], usually obtained with graphite as sacrificial additive and with the reduction of nickel oxide used to obtain the cermet YSZ-Ni.

In this work the use of potassium iodide, a low cost alkali halide, is proposed for the preparation of zirconia:8 mol% yttria as a first step for further development of porous zirconia-yttria/nickel cermets for solid oxide fuel cells.

Experimental

Zirconia-yttria (ZrO_2:8 mol% Y_2O_3 - 8YSZ) with 1.0, 2.0, 3.0, 5.0 and 10.0 wt.% of KI were prepared by thoroughly mixing and homogenizing in a pre-warmed agate mortar. The powders were pressed with ~ 400 kgf (10 mm diameter) followed by isostatic pressing at 30000 psi. Sintering was carried out at 1400 ^oC/2 h with a heating rate of 5 degree/min, with a previous heating at 690 ^oC for melting the potassium iodide for wetting the YSZ particles. Geometrical density and density using the Archimedes technique were evaluated.

Thermogravimetric analysis was carried out in a Netzsch STA 402E equipment from room temperature to 1200 ^oC, heating rate 5 degree/min. An 1161 Anter dilatometer was used for analysis of the shrinkage behavior in the room temperature - 1500 ^oC range.

X-ray fluorescence analysis was performed in a Shimadzu EDX-720 equipment for evaluation of remaining KI content in the sintered zirconia-yttria specimens.

X-ray diffraction experiments were carried out in a Bruker-AXS D8 Advance diffractometer with Cuk_α radiation under 40 kV, 40 mA, in the 20º-80º range, step 0.05º and time per step 2s.

Topographical images of polished and thermally etched surfaces of the pellets were obtained in a scanning probe microscope Jeol JSPM-5200 and in the FEG-SEM FEI Inspect F50 electron scanning microscope.

The electrical behavior was analyzed by impedance spectroscopy in the 5 Hz-13 MHz frequency range from 300 ºC to 450 ºC in a Hewlett Packard 4192A impedance analyzer. A special software was used for collecting and analyzing the [-Z''(ω) x Z'(ω)] data [11].

Results and Discussion

Figure 1 shows the results of the thermogravimetric analysis of ~ 50 mg of 8YSZ powders mixed to 1.0, 2.0, 5.0 and 10.0 wt.% KI. Mass loss of 0.0, 1.1, 1.3, 4.0 and 10.0% for x=1.0, 2.0, 5.0, and 10.0 occurs in the 700-800 ^oC range, due to KI loss after melting.

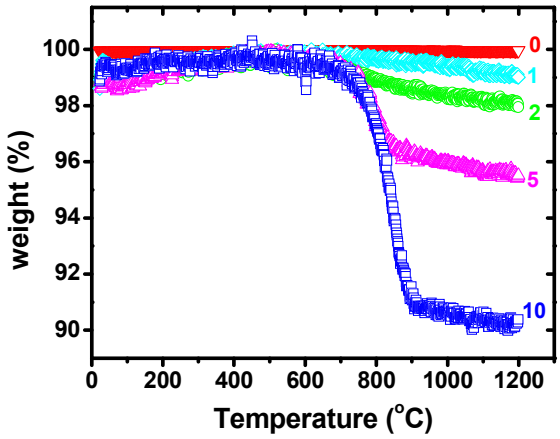

Figure 1. Thermogravimetric curves of ZrO_2: 8 mol% Y_2O_3 + x wt.% KI, x = 0, 1.0, 2.0, 5.0 and 10.0.

The dilatometric curves of all pressed pellets are shown in Figure 2. The larger is the KI content added to 8YSZ, the lower is the final attained shrinkage. This might be due a decrease in the diffusion coefficient of the oxide ion vacancies at the intergranular regions by the presence of the molten potassium iodide. The fitting of the derivative of the curves yields the following values for the maximum shrinkage temperatures : 1352 ºC, 1366 ºC , 1322 ºC, 1372 ºC and 1350 ºC for 0, 1.0, 2.0, 3.0, 5.0 and 10.0 wt.% nominal content of KI, respectively.

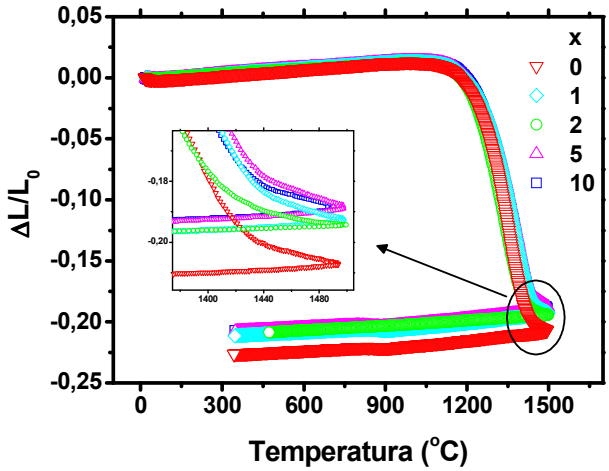

Figure 2. Shrinkage as a function of the temperature during heating ZrO_2: 8 mol% Y_2O_3 + x wt.% KI, $0 \leq x \leq 10$. Insert shows a zoom in the 1380 ºC - 1500 ºC range.

The evaluation of the iodine content in the pre-sintered specimens by XRF analysis yielded 0,1.3, 1.9, 4.3 and 8.8 wt.% for x=0, 1.0, 2.0, 3.0, 5.0 and 10.0, respectively. After sintering, none of the specimens showed any iodine content.

The relative hydrostatic densities of all specimens were 97.8%, 96.8%, 96.0%, 93.4% and 89.0% of the theoretical density for KI additions of 0, 1.0, 2.0, 3.0, 5.0 and 10.0 wt.%, respectively.

The X-ray diffraction patterns of all specimens show that the crystalline phase is the cubic fluorite phase with the main indexed reflections at (111), (200), (220), (311), (222) and (400) planes.

Figure 3 shows [-Z" (ω) x Z' (ω)] impedance diagrams of ZrO_2 : 8 mol% Y_2O_3 without and with additions of KI, measured at 320 ºC in the 5 Hz-13 MHz frequency range. Two well resolved semicircles, due to the bulk (high frequencies) and to grain boundaries (low) are evident.

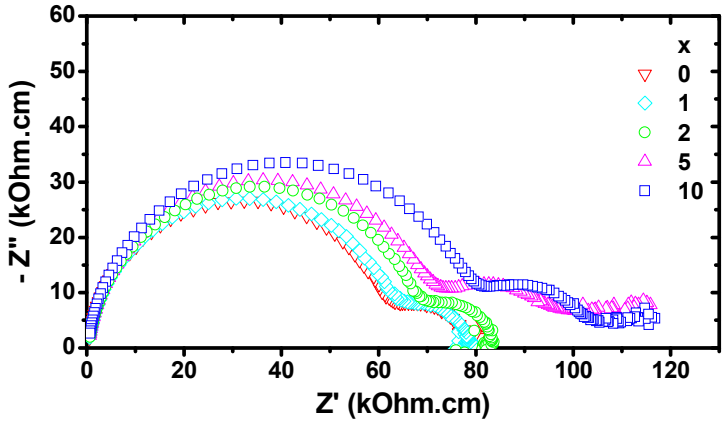

Figure 3. Impedance plots of ZrO_2: 8 mol% Y_2O_3 + x wt.% KI, x=0, 1.0, 2.0, 5.0 and 10.0, measured at 320ºC.

The deconvolution of the impedance semicircles due to intragranular and intergranular contributions to the electrical resistivity shows that both components increase with increasing KI content, meaning that pores might be located at the grains as well as at the grain boundaries.

Next we show the images observed at the polished and etched surfaces of the sintered specimens without and with addition of KI. Figure 4 shows at the left the micrographs observed in the FEG-SEM microscope and at the right the ones observed at the scanning probe microscope. A preliminary evaluation shows that the pore content increases consistently with the increase of the potassium iodide mixed to the 8YSZ solid electrolyte, whereas the average grain size decreases.

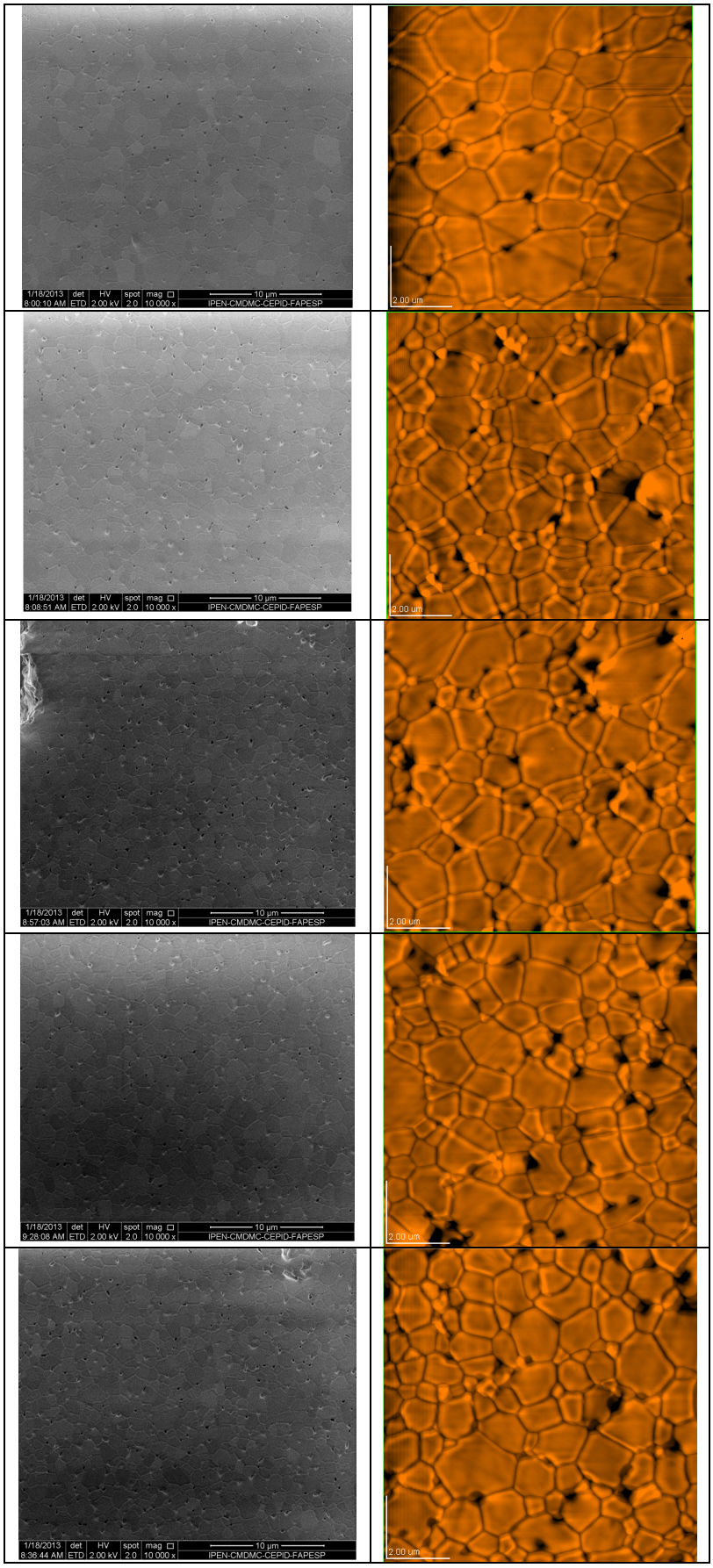

Figure 4. SEM and SPM micrographs of polished and etche surfaces of ZrO_2: 8 mol% Y_2O_3 + x wt.% KI, x = 0, 1.0, 2.0, 5.0 and 10.0, from top to bottom.

Conclusions

Porous ceramic solid electrolytes of composition 8 mol% yttria-stabilized zirconia have been prepared by addition and thermal removal of potassium iodide. Skeletal densities in the 89-98% of the theoretical density were obtained. Impedance spectroscopy analysis of the sintered pellets as well as scanning probe microscopy and scanning electron microscopy observation of their surfaces show that the porosity may be controlled by suitable addition/removal of potassium iodide. As expected, the pore content increases for increasing amount of potassium iodide added prior to sintering. The impedance spectroscopy results show the increase in the bulk as well as in the intergranular resistivity due to pore formation both inside the grains and at the grain boundaries.

Acknowledgements

To CNEN, FAPESP (Procs. 2005/53241-9 and 2013/08435-6) and CNPq (Procs. 471885/2010-0 and 303414/2009-0) for financial support. To Dr. J. R. Martinelli for the X-ray fluorescence analysis.

References

[1] P. Colombo, In praise of pores, Science 322 (2008) 381-383.
[2] R. W. Rice, Ceramic fabrication technology, Marcel Dekker, New York, 2003
[3] J. Saggio-Woyansky, C. E. Scott, W. P. Minnaer, Processing of porous ceramics, Am. Ceram. Soc. Bull 71 (1992) 1674-1682.
[4] L. Dessemond, R. Muccillo, M. Henault, M. Kleitz, Electric conduction-blocking effects of voids and second phases in stabilized zirconia, Appl. Phys. A 57 (1993) 57-60.
[5] M. Kleitz, L. Dessemond, M. C. Steil, Model for ion-blocking at internal surfaces in zirconias, Solid State Ionics 75 (1995) 107-115.
[6] X. Guo, Physical origin of the intrinsic grain-boundary resistivity of stabilized zirconia. Role of space charge layers, Solid State Ionics 81 (1995) 235-242.
[7] M. Kleitz, C. Pescher, L. Dessemond, Impedance spectroscopy of microstructure defects and crack characterization, in S. P. S. Badwal, M. J. Bannister, R. J. H. Hannick (Eds.), Science and Technology of Zirconia V, Technomic Publ. Co. Inc., 1993, p.593.
[8] R. Muccillo, Impedance spectroscopy analysisd of zirconia: 8 mol% yttria solid electrolytes with graphite pore former, J. Mater. Res. 24 (2009) 1780-1784.
[9] T. Suzuki, Z. Hasan, Y. Funahashi, T. Yamaguchi, Y. Fujishiro, M. Awano, Impact of anode microstructure on solid oxide fuel cells, Science 325 (2009) 852-855.
[10] E. W. Park, H. Moon, M. S. Park, S. H. Hyun, Fabrication and characterization of Cu-Ni-YSZ SPFC anodes for direct use of methane via Cu-electroplating, Int. J. Hydrogen Energy 34 (2009) 5537-5545.
[11] M. Kleitz, J. H. Kennedy, Resolution of multicomponents impedance diagrams. in P. Vashishta, J. N. Mundy, G. K. Shenoy (Eds.), Proc. Int. Conf. on Fast Ion Transport in Solids, Electrodes and Electrolytes, North-Holland, Amsterdam, 1979, p.1858.